

1 **Impacts of anthropogenic water regulation on global** 2 **riverine dissolved organic carbon transport**

3 Yanbin You^{1,2}, Zhenghui Xie^{1,2*}, Binghao Jia^{1*}, Yan Wang³, Longhuan Wang¹, Ruichao
4 Li¹, Heng Yan^{1,2}, Yuhang Tian^{1,2}, Si Chen^{1,2}

5 ¹State Key Laboratory of Numerical Modeling for Atmospheric Sciences and Geophysical Fluid
6 Dynamics, Institute of Atmospheric Physics, Chinese Academy of Sciences, Beijing 100029, China

7 ²College of Earth and Planetary Sciences, University of Chinese Academy of Sciences, Beijing 100049,
8 China

9 ³State Key Laboratory of Hydrology-Water Resources and Hydraulic Engineering, Nanjing Hydraulic
10 Research Institute, Nanjing 210029, China

11 *Correspondence to:* Zhenghui Xie (zxie@lasg.iap.ac.cn), Binghao Jia (bhjia@mail.iap.ac.cn)

12 **Abstract.** Anthropogenic water regulation activities, including reservoir interception, surface water
13 withdrawal, and groundwater extraction, alter riverine hydrologic processes and affect dissolved organic
14 carbon (DOC) export from land to rivers and oceans. In this study, schemes describing soil DOC leaching,
15 riverine DOC transport, and anthropogenic water regulation were developed and incorporated into the
16 Community Land Model 5.0 (CLM 5.0) and the River Transport Model (RTM). Three simulations by the
17 developed model were conducted on a global scale from 1981 to 2013 to investigate the impacts of
18 anthropogenic water regulation on riverine DOC transport. The validation results showed that DOC
19 exports simulated by the developed model were in good agreement with global river observations. The
20 simulations showed that DOC transport in most rivers was mainly influenced by reservoir interception
21 and surface water withdrawal, especially in central North America and eastern China. Four major rivers,
22 including the Danube, Yangtze, Mississippi, and Ganges Rivers, have experienced reduced riverine DOC
23 flows due to intense water management, with the largest effect occurring in winter and early spring. In
24 the Danube and Yangtze River basins, the impact in 2013 was four to five times greater than in 1981,
25 with a retention efficiency of over 50 %. The Ob River basin was almost unaffected. The total impact of
26 anthropogenic water regulation reduced global annual riverine DOC exports to the ocean by
27 approximately $13.36 \pm 2.45 \text{ Tg C yr}^{-1}$, and this effect increased from 4.83 % to 6.20 % during 1981–
28 2013, particularly in the Pacific and Atlantic Oceans.

29 **1. Introduction**

30 Rivers are a pipe linking the two major carbon pools of terrestrial and ocean ecosystems and are one of
31 the key hubs of the global carbon cycle (Cole et al., 2007). According to the Fifth Assessment Report of
32 the Intergovernmental Panel on Climate Change (IPCC AR5), terrestrial ecosystems deliver about 1.7 Pg
33 C per year to rivers through surface and subsurface runoff and about 0.9 Pg C per year to oceans via
34 rivers. Approximately 0.21 Pg of this is dissolved organic carbon (DOC) (Ludwig et al., 1996), which is
35 equivalent to about 1 % of the global net primary productivity (NPP) of terrestrial ecosystems (Zhang,
36 2012). Riverine DOC is a rather highly reactive organic carbon, easily decomposed. It is a direct source
37 of carbon for microbial food webs in rivers and oceans, as well as a source of greenhouse gas emissions
38 from freshwater systems (Li et al., 2019; Tranvik & Jansson, 2002). It deeply affects the biogeochemical
39 cycles of rivers and offshore ecosystems. Therefore, it is important to clarify the transport characteristics
40 of riverine DOC for estimating global carbon budgets.

41 In recent years, anthropogenic water management activities, including reservoir interception, surface
42 water withdrawal, and groundwater extraction, have intensified the degree of interference with natural
43 processes on the surface of river basins, altered the hydrological and hydraulic processes of rivers, and
44 affected material circulation and transportation (Zhang, 2012). For example, extraction from
45 underground aquifers affects hydrological systems, leading to a reduction in subsurface runoff and
46 eventually to decreased soil carbon losses (Zeng et al., 2016). Whereas activities such as irrigation can
47 lead to increased surface runoff, resulting in increased soil carbon losses (Ren et al., 2016). Artificially
48 constructed large reservoirs or dams disrupt the carbon cycle balance of the river continuum in its natural
49 state (Maavara et al., 2017), resulting in retention of DOC and sediment, while lower river velocities and
50 higher material concentrations lead to increased microbial activity in the water body, thus changing the
51 nutrient state of the river ecosystem (Liu et al., 2022). However, the impact of these anthropogenic
52 disturbances on riverine carbon transport has been ignored in estimating the global carbon budget
53 (Regnier et al., 2013).

54 Based on field surveys involving global riverine DOC transport flux estimation, the United Nations
55 Environment Programme has constructed a world river discharge database, GEMS-GLORI, that lists 48
56 attributes of 555 major world rivers (Meybeck, 1982; Meybeck & Ragu, 2012). There are also regional
57 survey programs, such as the Pan-Arctic River Transport of Nutrients, Organic Matter, and Suspended

58 Sediments (PARTNERS, <https://arcticgreatrivers.org/>) and the United States Geological Survey (USGS)
59 Data Center (<https://waterdata.usgs.gov/nwis>), which provide riverine organic carbon flux data for parts
60 of large rivers. Field survey studies are directly limited by data availability and completeness and
61 therefore mostly focus on large rivers in developed regions, making it difficult to cover rivers in other
62 regions. Moreover, only annual averages are usually available, with no long-term time series variation.
63 Some researchers have started to explore the mechanisms of riverine carbon flux changes using empirical
64 statistical models, which combine observed data with driving factors including river basin characteristics
65 (Ludwig et al., 1996), soil carbon and nitrogen ratios (Aitkenhead & McDowell, 2000), land-cover types
66 (Harrison et al., 2005), and river discharge (Fabre et al., 2020). However, the empirical statistical method
67 does not consider complex ecological processes within the watershed and cannot describe material
68 changes in the river network in detail. To identify changes in carbon transport and its driving mechanisms
69 spatially and explicitly, numerous process-based numerical models are currently used for DOC transport
70 simulations. Futter et al. (2007) proposed the integrated catchments model for carbon (INCA-C), which
71 explicitly considers land use, hydrological processes, soil carbon biogeochemical cycles, and surface
72 water processes. Liao et al. (2019) developed a three-dimensional terrestrial ecosystem model (ECO3D)
73 considering the influence of lateral water flows. These models simulate regional riverine DOC dynamics
74 more accurately than earlier models, but their accuracy relies on complex parametric schemes of eco-
75 hydrological processes and extensive data surveys, so that it is difficult to extend these models to global-
76 scale simulations. Wu et al. (2014) integrated ecological driving factors and biogeochemical processes
77 to develop a TRIPLEX-DOC model that predicts DOC metabolism, sorption, desorption, and loss
78 processes in soils. Li et al. (2019) added a river hydrological process module to construct the TRIPLEX-
79 HYDRA model and applied it to simulate global riverine DOC fluxes. However, the model did not
80 consider the impact of human activities on riverine DOC transport. Tian et al. (2015) constructed the
81 dynamic land ecosystem model (DLEM), a fully distributed model that integrates vegetation dynamics
82 with processes such as water, carbon, nitrogen, and phosphorus cycling and the effects of human activities
83 and climate change to simulate DOC flux transport in eastern North American rivers. To better quantify
84 riverine carbon transport processes at watershed scale, Yao et al. (2021) coupled the scale-adaptive water
85 transport model (Li et al., 2013) to the DLEM model and applied the result to two mid-Atlantic
86 watersheds in the United States. Nevertheless, these models failed to consider the effects of

87 anthropogenic water regulation activities. Furthermore, constructing numerical simulation models is a
88 future development direction of riverine carbon flux estimation; at present, models are still not widely
89 used to simulate riverine carbon transport (Camino-Serrano et al., 2018).

90 In this study, we incorporated global soil and riverine DOC transport schemes considering
91 anthropogenic water regulation activities into Community Land Model 5.0 (CLM5.0) and conducted
92 numerical simulations at global scale (spatial resolution of about 1° for the land processes and 0.5° for
93 the river systems) during 1981–2013 to explore the impact of anthropogenic water regulation activities
94 on land-to-ocean riverine DOC transport.

95 **2. Model Development**

96 **2.1. Model Overview**

97 The model was developed based on CLM5.0, which is the land component of the CESM (Community
98 Earth System Model). CLM is widely used to simulate and study land surface ecohydrological processes,
99 surface energy exchange processes, and other biogeochemical processes. The latest version of CLM
100 updates most components of previous versions, explicitly represents land-use and land-cover change,
101 introduces a revised canopy interception parameterization, and significant improvements in soil layer
102 resolution, nitrogen cycle, and the snow model. Moreover, CLM5.0 includes two river routing methods:
103 the Model for Scale Adaptive River Transport (MOSART, Li et al., 2013) and the River Transport Model
104 (RTM). Because the scale of this study was global, the routing method still uses linear scheme RTM.

105 However, CLM5.0 lacks an expression of the soil DOC leaching process and the DOC transport and
106 transformation process in rivers. Therefore, in this paper, schemes for DOC leaching in soils and DOC
107 transport in rivers will be proposed and incorporated into CLM5.0 to simulate riverine carbon transport.
108 To investigate the effect of anthropogenic water regulation activities on global riverine DOC transport,
109 this study used the scheme proposed by Zeng et al. (2016), and coupled it with DOC transport processes.
110 The model framework is shown in Fig. 1.

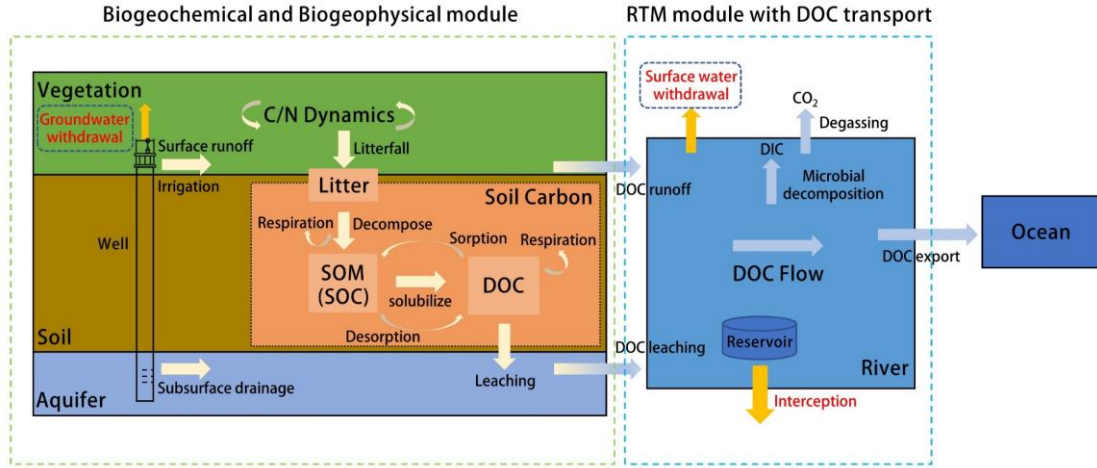


Figure 1. Schematic diagram of the land surface model with riverine dissolved organic carbon (DOC) transport and anthropogenic water regulation (C: carbon; N: nitrogen; SOM: soil organic matter; SOC: soil organic carbon; DIC: dissolved inorganic carbon).

111 2.2. Soil DOC loss to the river

112 Riverine DOC is mainly derived from organic carbon leaching processes in soil ecosystems in the
 113 watershed (Gommet et al., 2022; Li et al., 2019). In CLM5.0, only the leaching process of soil mineral
 114 nitrogen is included, and therefore a DOC production and loss process was introduced in this study. The
 115 soil biochemistry module in CLM5.0 was constructed based on the Century model (Parton et al., 1988),
 116 in which the decomposition of fresh litter into soil organic matter is defined as a transformation cascade
 117 between the coarse woody debris (CWD) pool, the litter pool, and the soil organic matter (SOM) pool.
 118 The NPP produced by plants eventually enters the soil in the form of litter to constitute the soil carbon
 119 pool, accompanied by an intervening loss through microbial heterotrophic respiration. Assuming that
 120 dissolved organic matter (DOM) production is part of the turnover of litter pools and soil organic matter
 121 pools and is proportional to soil water content, DOC production can be expressed as (Gerber et al., 2010):

$$122 \quad P_{DOC,u \rightarrow d} = f_{DOM} \theta CF_{u \rightarrow d}, \quad (1)$$

123 where $P_{DOC,u \rightarrow d}$ ($\text{g C m}^{-2} \text{s}^{-1}$) is the DOC flux from the decomposition process; f_{DOM} is the fraction
 124 that enters the soil DOM pool; θ ($\text{m}^3 \text{m}^{-3}$) is the soil water content; and $CF_{u \rightarrow d}$ ($\text{g C m}^{-2} \text{s}^{-1}$) is the
 125 carbon flux from upstream to downstream carbon pools in the decomposition cascade.

126 Soil organic carbon remaining after plant growth and soil respiration is subject to loss as a dissolved
 127 component leaching from the soil column. In this study, the DOC runoff is defined as the soil DOC in
 128 surface runoff, and the DOC leaching is defined as the subsurface losses of DOC in soil water. The fluxes
 129 are described as follows:

130
$$DOC_{runoff} = [DOC]Q_{surf}k_{adsorb} - SR, \quad (2)$$

131
$$DOC_{leaching} = [DOC]Q_{dis}k_{adsorb} - SR, \quad (3)$$

132 where DOC_{runoff} ($\text{g C m}^{-2} \text{ s}^{-1}$) denotes the soil DOC runoff, $DOC_{leaching}$ ($\text{g C m}^{-2} \text{ s}^{-1}$) denotes the soil
 133 DOC leaching, Q_{surf} ($\text{kgH}_2\text{O m}^{-2} \text{ s}^{-1}$) denotes the surface runoff, Q_{dis} ($\text{kgH}_2\text{O m}^{-2} \text{ s}^{-1}$) denotes the
 134 subsurface discharge, $[DOC]$ ($\text{g C kgH}_2\text{O}^{-1}$) is the DOC concentration in the soil water solution:

135
$$[DOC] = \frac{NS_{DOC}}{WS_{tot_soil}}, \quad (4)$$

136 where WS_{tot_soil} ($\text{kgH}_2\text{O m}^{-2}$) is the total mass of soil water content integrated over the soil column and
 137 NS_{DOC} (g C m^{-2}) is the DOC in the soil pool.

138 Soil DOC readily complexes with metal ions in the soil and forms soil agglomerates, which enable
 139 soil DOC to be adsorbed onto soil particles. The DOC adsorption coefficients can be estimated as (Li et
 140 al., 2019; Neff & Asner, 2001):

141
$$k_{adsorb} = \frac{X_i}{X_i + RE}, \quad (5)$$

142
$$RE = mX_i - b, \quad (6)$$

143 where X_i (mg g soil^{-1}) represents the initial DOC concentration, RE (mg g soil^{-1}) is the amount of DOC
 144 desorbed (negative value) or adsorbed (positive value), calculated by the simple initial mass (IM) linear
 145 isotherm, m (dimensionless coefficient) and b (mg g soil^{-1}) can be considered as measures of potential
 146 DOC sorption and desorption by soil.

147 The soil heterotrophic respiration flux of DOC, SR ($\text{g C m}^{-2} \text{ s}^{-1}$), is estimated by an empirical function
 148 (Janssens and Pilegaard, 2003):

149
$$SR = R_{10}Q_{s10} \frac{T-10}{10}, \quad (7)$$

150 where T ($^{\circ}\text{C}$) is the soil temperature; R_{10} is the soil heterotrophic respiration flux at a soil temperature of
 151 10°C ; Q_{s10} is the soil respiration temperature sensitivity.

152 It is necessary to limit the total DOC runoff/leaching flux at each time step so that it does not exceed
 153 the total amount of DOC:

154
$$DOC_{loss} = \min(DOC_{loss}, \frac{NS_{DOC}}{\Delta t}). \quad (8)$$

155 where DOC_{loss} ($\text{g C m}^{-2} \text{ s}^{-1}$) denotes the soil DOC runoff or leaching.

156 2.3. Riverine DOC transport

157 Soil DOC enters the river network system along with surface and subsurface runoff, where it is lost due
158 to processes such as microbial degradation. Therefore, based on the water transport framework, the large-
159 scale riverine DOC transport equation can be defined as:

$$160 \quad \frac{dS_{DOC}}{dt} = F_{DOC}^{in} - F_{DOC}^{out} + R_{DOC} + L_{DOC} - k_{doc} * Q_{10}^{\frac{rt-20}{10}} * S_{DOC}, \quad (9)$$

161 where S_{DOC} (kg C) is DOC storage within the current grid cell; R_{DOC} (kg C s⁻¹) and L_{DOC} (kg C s⁻¹)
162 represent soil DOC runoff and leaching; k_{doc} (s⁻¹) is the DOC decomposition rate in the river; Q_{10}
163 (=2.0) denotes the temperature coefficient; rt (°C) represents the river water temperature, which is
164 calculated by a large-scale river water temperature model (Liu et al., 2020; van Vliet et al., 2012; Yearsley,
165 2009); F_{DOC}^{in} (kg C s⁻¹) is the sum of inflows of riverine DOC from neighboring upstream grid cells;
166 and F_{DOC}^{out} (kg C s⁻¹) is the riverine DOC flux leaving the current grid cell, which is calculated as follows:

$$167 \quad F_{DOC}^{out} = \frac{vS_{DOC}}{d}, \quad (10)$$

$$168 \quad v = \max(0.05, \beta^{1/2}), \quad (11)$$

169 where v (m s⁻¹) is the effective riverine flow velocity, which is estimated by grid cell mean topographic
170 slope β (Oleson et al., 2013); d is the Euclidean distance between two adjacent grid-cell centers.

171 2.4. Anthropogenic water regulation

172 Anthropogenic water regulation includes reservoir interception, surface water withdrawal, and
173 groundwater extraction and use. Because reservoir interception and surface water withdrawal are closely
174 related, they are together called surface water regulation. This study coupled the global reservoir
175 operation scheme (Hanasaki et al., 2006) with RTM using the method of Liu et al. (2019) to represent
176 the interception effect of reservoirs on runoff and solutes. The method assumed that the inflow from the
177 reservoir was the outflow from the current grid cell. Released flow from the reservoir was adjusted for
178 specific uses (flood control, irrigation, etc.), and surface withdrawals were deducted from the released
179 water (see Sect. S1 in the Supplement).

180 Surface water is extracted directly from natural rivers and reservoirs to meet human water demands
181 (Wang et al., 2020; Xie et al., 2020; Liu et al., 2019):

$$182 \quad S_{sw}' = S_{sw} - q_{sw}\Delta t, \quad (12)$$

183 where S_{sw}' (mm) is the surface water storage after extraction; S_{sw} (mm) is the original surface water

184 storage; q_{sw} (mm s^{-1}) is the rate of surface water intake; Δt denotes the model time step.

185 The groundwater extraction process can be expressed as (Zeng et al., 2016):

186
$$S_{gw}' = S_{gw} - q_{gw}\Delta t, \quad (13)$$

187
$$h' = h - \frac{q_{gw}\Delta t}{s}, \quad (14)$$

188 where S_{gw} (mm) is the original unconfined aquifer water storage; q_{gw} (mm s^{-1}) is the rate of
189 groundwater pumping; h (mm) represents the original groundwater table depth; s is the aquifer-
190 specific yield; S_{gw}' (mm) and h' (mm) denote the aquifer water storage and the groundwater table depth
191 after pumping.

192 Human water use can be divided into agricultural irrigation water and other industrial and domestic
193 water, where irrigation water is considered as effective precipitation directly back to the soil surface and
194 other water is directly added to the model surface runoff and evapotranspiration fluxes in a certain
195 proportion (Zou et al., 2015). This process can be estimated by the following equations:

196
$$q_{top} = q_{top} + q_{irrig}, \quad (15)$$

197
$$q_{surf} = q_{surf} + 0.3q_{ind} + 0.3q_{dom}, \quad (16)$$

198
$$q_{evap} = q_{evap} + 0.7q_{ind} + 0.7q_{dom}, \quad (17)$$

199 where q_{top} (mm s^{-1}) is the rate of net water flow entering the soil surface; q_{surf} and q_{evap} (mm s^{-1}) are
200 surface runoff and evaporation; and q_{irrig} , q_{ind} , and q_{dom} (mm s^{-1}) denote irrigation, industrial, and
201 domestic water respectively. The coefficients were set to 0.3 and 0.7 due to the limitation of data (Liu et
202 al., 2019; Zou et al., 2014).

203 **2.5. DOC transfer induced by water withdrawal and use**

204 Anthropogenic water regulation activities also affect DOC transport processes between land and river. It
205 was assumed here that (1) only the interception effect of reservoirs would be considered, ignoring the
206 migration transformation process in reservoirs, and the loss rate in reservoirs would be equal to that in
207 rivers; (2) because groundwater extraction usually occurs *in situ* and will pass through the filtering effect
208 of the soil layer, the part of DOC that returned to soil with groundwater extraction was ignored; (3) the
209 loss rate in the process of DOC returning to soil was equal to that in rivers.

210 The process of reservoir interception leading to retention of carbon in rivers can be expressed as:

211
$$F_{DOC,r} = \frac{v(con_r\Delta Q_r)}{d}, \quad (18)$$

212 where $F_{DOC,r}$ (kg C s⁻¹) denotes the DOC flux retained by the reservoir; con_r (kg C m⁻³) is the DOC
213 concentration in the reservoir; ΔQ_r (m³) is the water volume change in the reservoir. Therefore, the
214 riverine DOC flux leaving the current grid cell is updated to:

$$215 \quad F_{DOC}^{out} = F_{DOC}^{out} - F_{DOC,r}, \quad (19)$$

216 The DOC flux extracted from surface water is calculated based on the intake rate and the solute
217 concentration con_{DOC} (kg C m⁻³) in the current grid cell and return to the soil DOC pool after irrigation:

$$218 \quad F_{DOC}^{out} = F_{DOC}^{out} - q_{sw} con_{DOC}, \quad (20)$$

219 The reduction in soil DOC leaching due to groundwater extraction is then calculated based on soil
220 DOC concentration and groundwater pumping rate:

$$221 \quad DOC_{leaching} = DOC_{leaching} - q_{gw}[DOC]. \quad (21)$$

222 **3. Data and Experimental Design**

223 **3.1. Data Sources**

224 The climate input forcing data set (0.5° × 0.5°) used for the model proposed in this study was obtained
225 from CRU-NCEP Version 7 (Viovy, 2018), including air temperature, humidity, incoming solar radiation,
226 precipitation, surface pressures, and surface winds. The basic land-surface datasets required to drive the
227 model were set up using the default CLM 5.0 settings with a spatial resolution of 0.9° × 1.25°; more
228 details are available in the technical notes (Lawrence et al., 2018). The global monthly mean atmospheric
229 CO₂ concentration dataset came from the NOAA/Earth System Research Laboratory
230 (<https://www.esrl.noaa.gov/gmd/ccgg/trends/global.html>).

231 Reservoir information was obtained from the Global Reservoir and Dam Database (GRanD, Lehner et
232 al., 2011), containing information on 6,862 dams and their associated reservoirs worldwide, and
233 interpolated to a spatial resolution of 0.5° × 0.5° (Fig. S2).

234 The human water use activity dataset was derived from the global long-term surface and groundwater
235 withdrawal dataset estimated by Liu et al. (2019). The dataset has a spatial resolution of 0.5° × 0.5° and
236 contains agricultural, industrial, and domestic water demands from 1958 to 2017. It was derived based
237 on five datasets: the water use dataset from the Food and Agricultural Organization (FAO), a shape file
238 data of national boundaries, the Global Map of Irrigation Areas, version 5 (GAMIP5; Siebert et al., 2013),
239 the historical monthly soil moisture levels and saturated soil moisture levels (Zeng et al., 2017), and the

240 FAO water information system for 2010, which contained the agricultural, industrial, and municipal
 241 water withdrawals.

242 3.2. Observation Data

243 Because there are few datasets of long time-series observations of DOC fluxes for large global rivers,
 244 annual averages were used to validate the model simulations. The dataset was derived from the database
 245 developed by Dai et al. (2012), which provides discharge and DOC flux observations for sites on the
 246 world's major large rivers. These sites were globally distributed and were influenced by various climatic
 247 and human activities.

Table 1. Summary of the main datasets used in this study

Dataset	Resolution	Time period	Data Source
CRU-NCEP V7 forcing	0.5°/6 hr	1981-2013	Viovy (2018)
Surface water and groundwater withdrawal and use	0.5°	1958-2017	Liu et al. (2019)
Reservoir information	Site	Around 2011	Lehner et al. (2011)
River discharge	Site	Annual before 2009	Dai et al. (2012)
DOC export	Site	Annual before 2009	Dai et al. (2012)

248 3.3. Experimental Design

249 To investigate the effect of anthropogenic water regulation on DOC transport in rivers, three sets of
 250 simulations were designed using the developed model (Table 2). The first simulation (CTL) was a control
 251 experiment without considering any anthropogenic water regulation activities. The second simulation
 252 (EXPA) only considered surface water regulation, and the last simulation (EXPB) considered all
 253 anthropogenic water regulation. All simulations were run from 1981 to 2013 with a spatial resolution of
 254 $0.9^\circ \times 1.25^\circ$ for the land-surface module and $0.5^\circ \times 0.5^\circ$ for the RTM. The results were output on a
 255 monthly scale. Before the formal numerical simulations, the 1901–1920 atmospheric forcing data cycle
 256 was used to drive the model without any anthropogenic water regulation as the spin-up run to reach an
 257 equilibrium state.

Table 2. Experimental design

Name	Period	Surface water regulation	Groundwater regulation
CTL	1981–2013	✗	✗
EXPA	1981–2013	✓	✗
EXPB	1981–2013	✓	✓

258 **4. Results**

259 **4.1. Model Evaluation**

260 Figure 2 shows the spatial distribution of multi-year average soil DOC losses, which are the sum of DOC
261 surface runoff and subsurface leaching. The results show that the global distribution of soil DOC losses
262 varied widely, especially in Russia and Southeast Asia, western Africa, and tropical South America,
263 where the losses exceeded $1.8 \times 10^4 \text{ kg C km}^{-2} \text{ yr}^{-1}$, whereas low runoff arid regions such as northwestern
264 China, India, and North Africa had the smallest soil DOC losses. The tropics and the temperate regions
265 of the Northern Hemisphere were the regions with the highest soil DOC losses, which is generally
266 consistent with previous studies (Harrison et al., 2005).

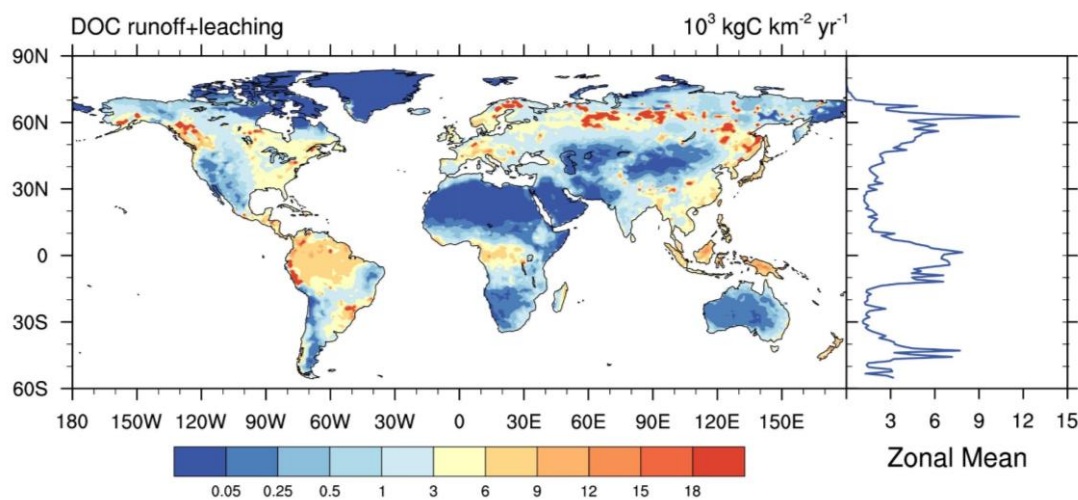


Figure 2. Spatial distribution and zonal mean of multi-year average soil DOC losses from 1981 to 2013.

267 The multi-year average river discharges and DOC export fluxes simulated by the developed model
268 were then compared with observed data. Because the model resolution was $0.5^\circ \times 0.5^\circ$, only 106 rivers
269 with watershed areas larger than $2,500 \text{ km}^2$ were selected. The simulated river discharges were slightly
270 underestimated (Fig. 3c), but fit well with observations (Fig. 3a) and provided a solid basis for subsequent
271 simulation of river carbon exports. In addition, the simulated riverine DOC export fluxes tended to be
272 overestimated in temperate regions and underestimated in the tropics (Fig. 3d), but were close to the 1:1
273 line compared to the observed DOC fluxes, with R^2 reaching 0.61 and significantly correlated (Fig. 3b).
274 Moreover, the total global river DOC export fluxes simulated by the proposed model were compared
275 with the results of previous studies. We estimated that the global terrestrial ecosystem delivers about

276 199.78 ± 36.63 (±1 standard deviation) Tg of DOC per year to the ocean via rivers, which was in the
 277 middle of the values derived from previous studies (Table 3). Therefore, it could be believed that the
 278 model has reasonable accuracy and can be applied to global-scale riverine DOC export simulation studies.

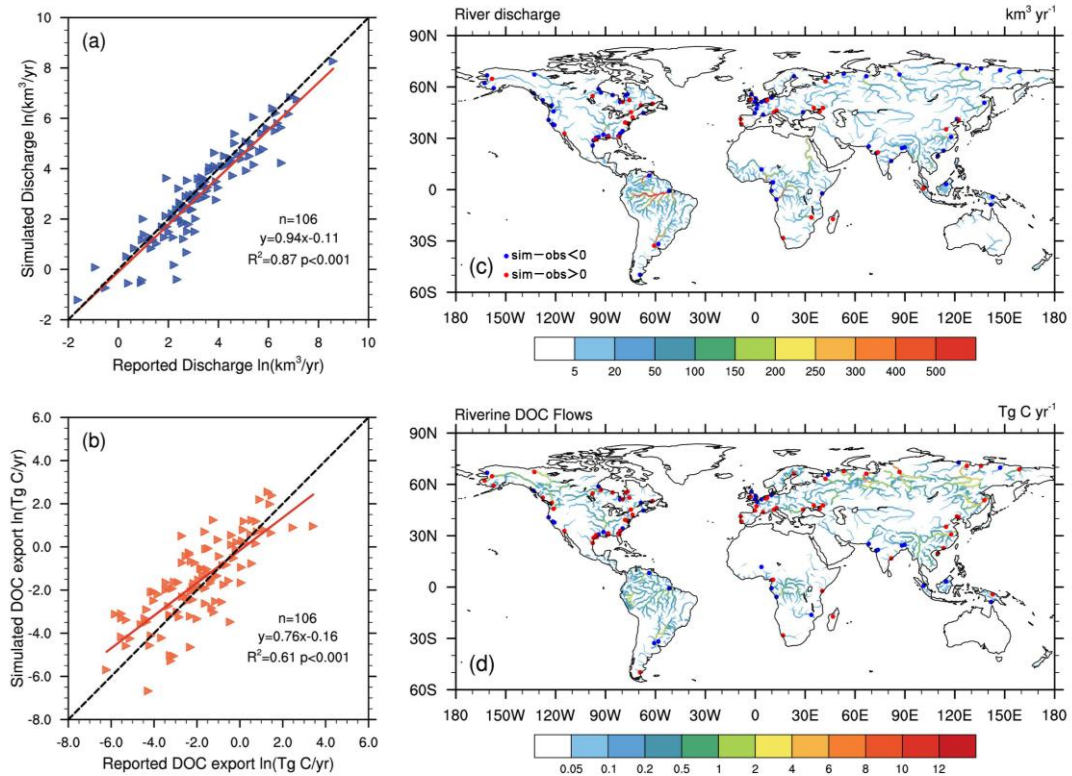


Figure 3. Simulated and reported annual (a) river discharge and (b) riverine DOC export flux for 106 global rivers. Spatial distributions of (c) annual discharge and (d) annual riverine DOC exports during 1981–2013. The dots in the map correspond to the locations of the 106 river sites, where blue dots indicate sites that are simulated underestimates and red dots indicate sites that are simulated overestimates.

Table 3. Comparison of simulated global total riverine DOC export fluxes with previous studies

Method	DOC (Tg C yr ⁻¹)	Data Source
GEMS-GLORI	215	Meybeck (1982)
Empirical model	204	Smith & Hollibaugh (1993)
Empirical model	204.81	Ludwig et al. (1996)
Global C: N	361	Aitkenhead & McDowell (2000)
NEWS-DOC	170	Harrison et al. (2005)
Global-NEWS	170	Seitzinger et al. (2005)
Statistical estimation	246	Cai (2011)
Statistical estimation	232.22	Drake et al. (2018)
TRIPLEX-HYDRA	240	Li et al. (2019)
Empirical model	131.6	Fabre et al. (2020)
DISC-CARBON	132	van Hoek et al. (2021)
CLM5.0-RTM	199.78	This study

279 4.2. Effects of surface water regulation on riverine DOC transport

280 The difference between EXPA and CTL was used to obtain the effect of surface water regulation on land
281 surface hydrological variables. Surface water use has resulted in changes in latent and sensible heat fluxes
282 in most global irrigation water-using regions (Fig. 4a, 4b), especially in arid or semi-arid regions such as
283 northern China, India, and the central United States, where latent heat fluxes have increased and sensible
284 heat fluxes have decreased. Soil and surface temperatures in these regions have also decreased due to the
285 cooling effect of irrigation (Fig. 4c, 4d). Figure 4e shows that irrigation led to an overall increase in soil
286 moisture, especially in northern India, Western Europe, and the midwestern United States. In addition,
287 irrigation also led to an increase in total runoff (Fig. 4f).

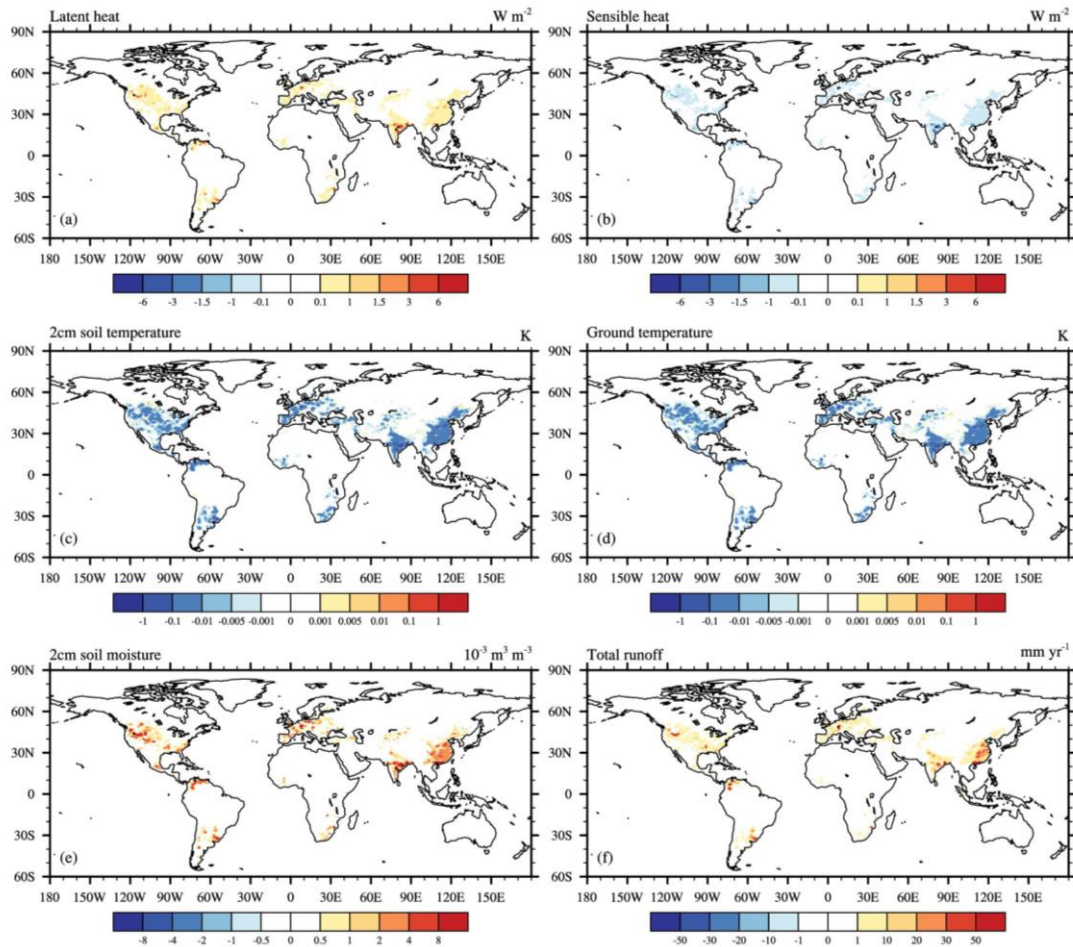


Figure 4. Spatial distribution of multi-year average differences in land surface hydrological variables between EXPA and CTL from 1981 to 2013: (a) latent heat flux, (b) sensible heat flux, (c) 2 cm soil temperature, (d) surface temperature, (e) 2 cm soil moisture, (f) total runoff. This figure demonstrates the effects of surface water regulation on land surface hydrological variables. The black dots are the regions that pass the significance *t*-test at the 95 % confidence level.

288 Figures 5a and 5b display the effects of surface water regulation on soil carbon losses. Specifically,
 289 the hotspots of significantly increased surface DOC runoff were in areas of high agricultural influence,
 290 such as the central United States, northern India, and northern and eastern China, reaching up to 2,000
 291 kg C km⁻² yr⁻¹, but the increase in subsurface leaching was relatively small. This may have been the case
 292 because surface water withdrawals from rivers and reservoirs were returned to the soil by irrigation,
 293 bringing back some DOC, directly increasing surface runoff, and also increasing subsurface runoff, and
 294 thus increasing soil DOC losses.

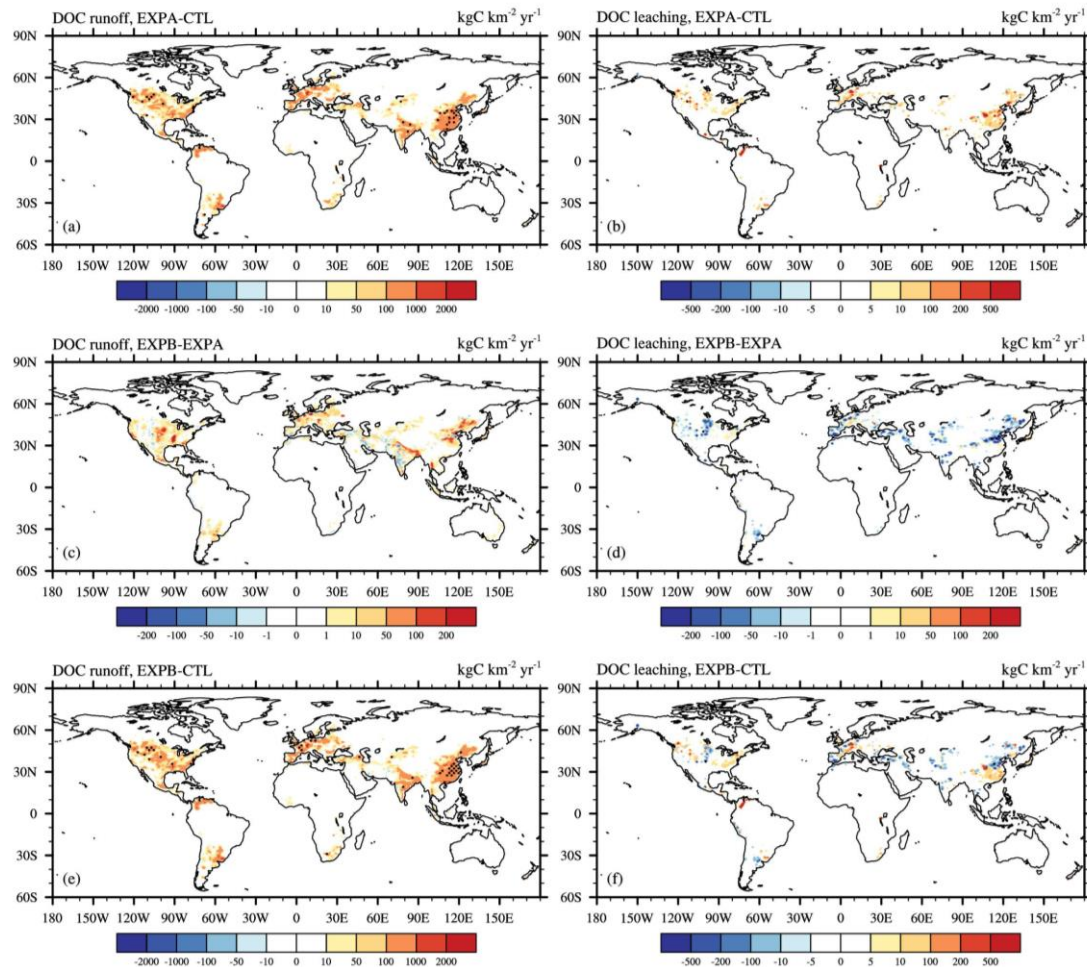


Figure 5. Spatial distribution of the multi-year average differences between different experiments from 1981 to 2013 in the (a) soil DOC runoff, EXPA–CTL, (b) soil DOC leaching, EXPA–CTL, (c) soil DOC runoff, EXPB–EXPA, (d) soil DOC leaching, EXPB–EXPA (e) soil DOC runoff, EXPB–CTL, (f) soil DOC leaching, EXPB–CTL. This figure demonstrates the effects of (a, b) surface water regulation, (c, d) groundwater regulation, and (e, f) anthropogenic water regulation on soil DOC losses. The black dots are the regions that pass the significance *t*-test at the 95 % confidence level.

295 From Fig. 6a and Fig. 6b, surface water regulation had a significant effect on river discharge and
 296 riverine DOC flow. The combined effects of reservoir interception and surface water withdrawal reduced
 297 the discharge and DOC export of most rivers globally, with significant reductions of more than 50 Gg C
 298 yr^{-1} in the Yangtze, Yellow, Mississippi, and Ganges Rivers and in some basins in Western Europe. Some
 299 rivers in northern South America experienced increased riverine DOC export, but not significantly,
 300 probably because the increase in river flow caused by agricultural irrigation could have been greater than
 301 the decrease caused by surface water regulation.

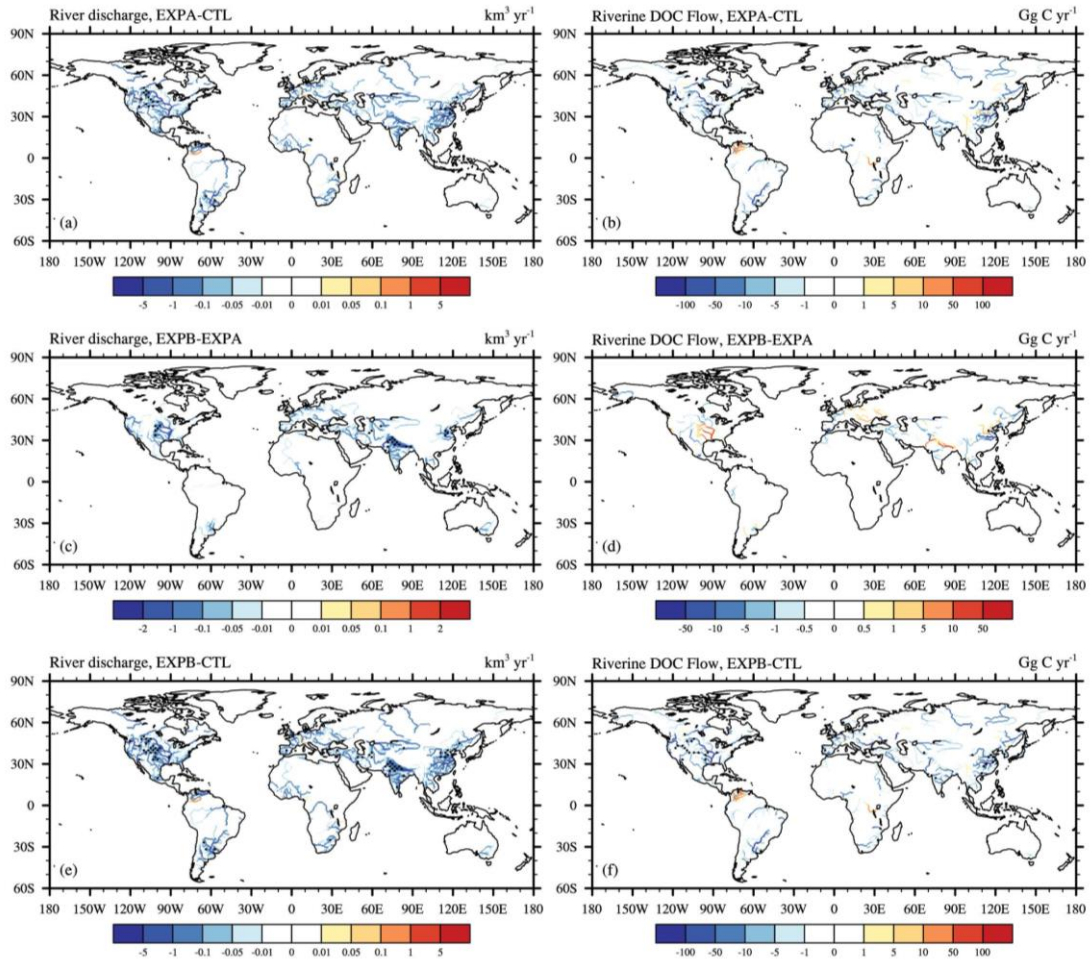


Figure 6. Spatial distribution of the multi-year average differences between different experiments from 1981 to 2013 in the (a) river discharge, EXPA-CTL, (b) riverine DOC flow, EXPA-CTL, (c) river discharge, EXPB-EXPA, (d) riverine DOC flow, EXPB-EXPA (e) river discharge, EXPB-CTL, (f) riverine DOC flow, EXPB-CTL. This figure demonstrates the effects of (a, b) surface water regulation, (c, d) groundwater regulation, and (e, f) anthropogenic water regulation on the river discharge and riverine DOC flow rate. The black dots are the regions that pass the significance *t*-test at the 95 % confidence level.

302 The blue line in Fig. 7 represents the time-series variation of surface water regulation on global riverine
 303 organic carbon to the ocean. Surface water regulation greatly reduced global riverine DOC transport to
 304 the ocean, from -11.1 Tg yr^{-1} in 1981 to -16.4 Tg yr^{-1} in 2013 (Fig. 7a), with a multi-year average
 305 retention efficiency of about 6 %. This may be related to the fact that the reservoir adjusting the river
 306 discharge and intercepting the riverine DOC. The regions most affected by surface water regulation were
 307 the Pacific and Atlantic Oceans, and as surface water use in these regions became more frequent, the
 308 reduction in DOC delivery to the ocean was intensified each year. There was no significant change in the
 309 Arctic Ocean region, which may have been due to less anthropogenic disturbance in this area.

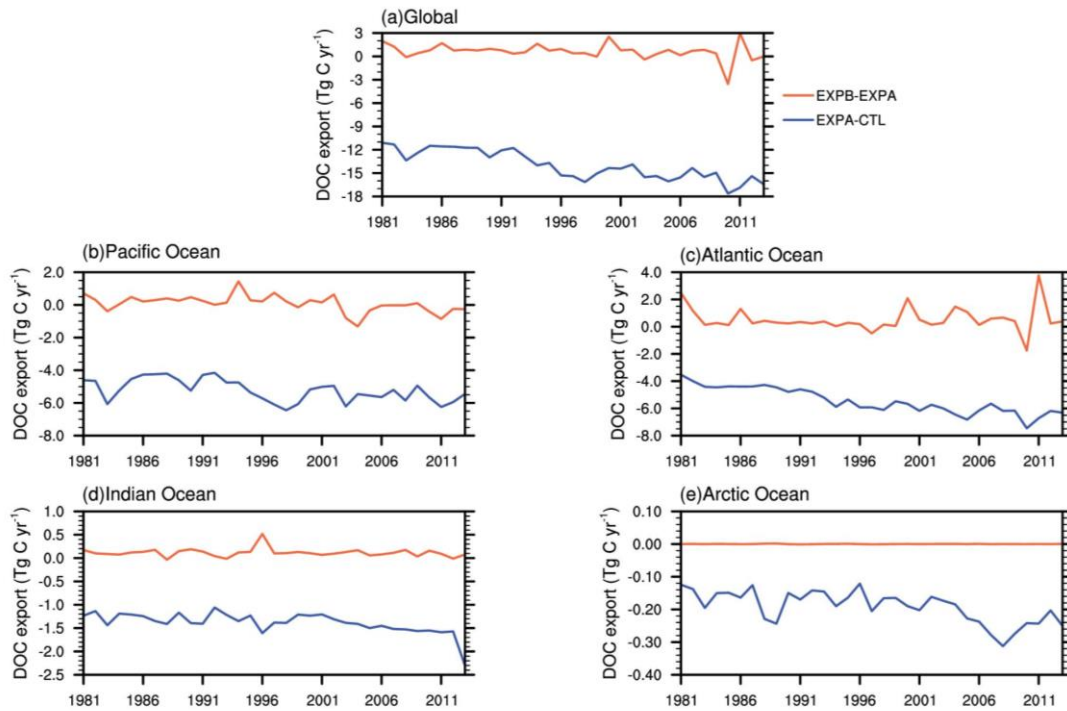


Figure 7. Time series of changes in DOC export to oceans due to surface water (blue line) and groundwater regulation (orange line) from 1981 to 2013: (a) global, (b) Pacific Ocean, (c) Atlantic Ocean, (d) Indian Ocean, (e) Arctic Ocean.

310 **4.3. Effects of groundwater regulation on riverine DOC transport**

311 The effects of groundwater regulation on land surface hydrological variables were obtained using the
 312 difference between EXPB and EXPA, as shown in Fig. 8. It can be seen that groundwater extraction
 313 increased latent heat fluxes, decreased sensible heat fluxes, decreased soil and surface temperatures, and
 314 increased soil moisture in most regions of the world. The most significant impacts were in northern China,
 315 northern India, Pakistan, and the central United States, where climate conditions are dry and groundwater
 316 extraction is frequent. Unlike surface water regulation, groundwater extraction has a negative impact on
 317 total runoff (Fig. 8f). Because groundwater is extracted from underground aquifers, whereas surface
 318 water is extracted from rivers and reservoirs, surface water use directly increases total land surface runoff.
 319 However, the impact of groundwater extraction on runoff depends on the groundwater pumping rate,
 320 infiltration rate, and soil evaporation capacity. The increase in latent heat flux leads to an increase in
 321 surface evapotranspiration, which results in a decrease in runoff.

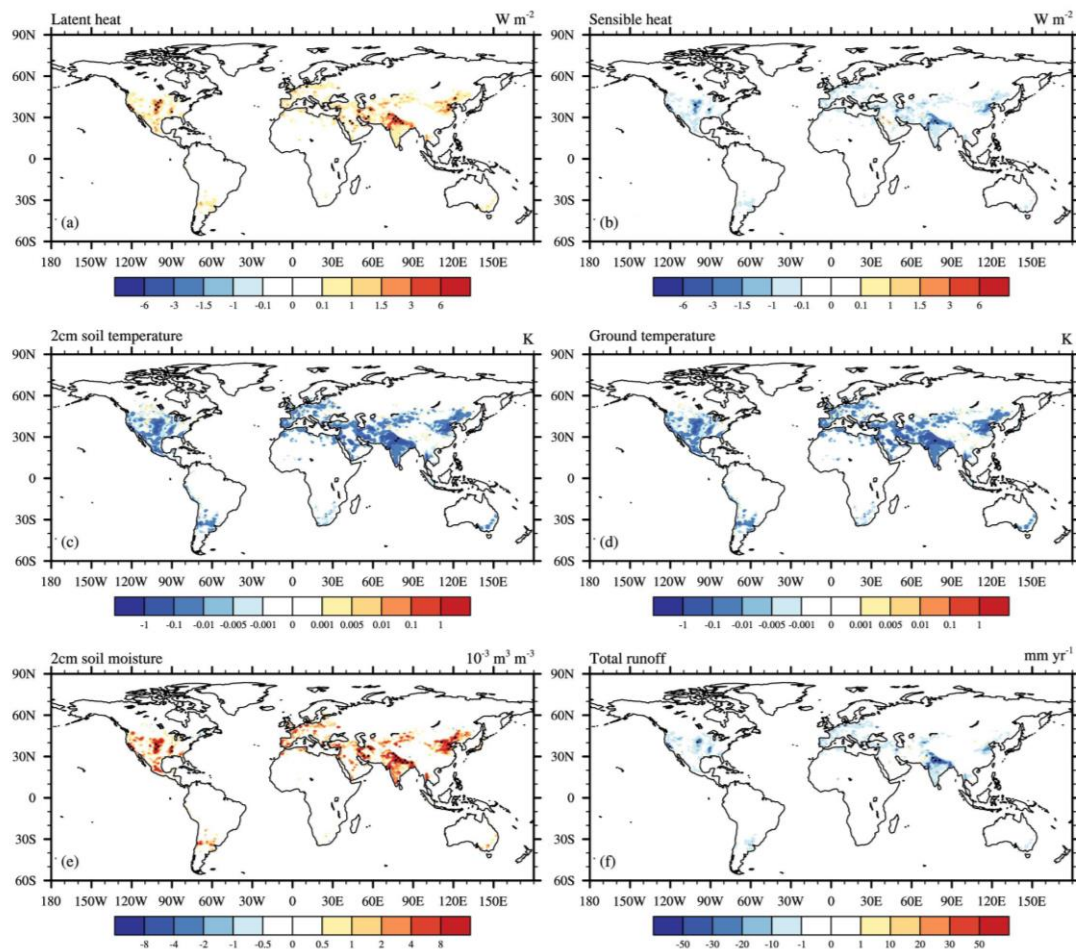


Figure 8. Spatial distribution of multi-year average differences in land surface hydrological variables between EXPB and EXPA from 1981 to 2013: (a) latent heat flux, (b) sensible heat flux, (c) 2 cm soil temperature, (d) surface temperature, (e) 2 cm soil moisture, (f) total runoff. This figure demonstrates the effects of groundwater regulation on land surface hydrological variables. The black dots are the regions that pass the significance *t*-test at the 95 % confidence level.

322 Figures 5c and 5d show the effect of groundwater regulation on soil carbon losses. On the one hand,
 323 extracting water from underground aquifers led to a reduction in subsurface runoff and a consequent
 324 reduction in DOC leaching, especially in northern China and the central United States, where DOC
 325 leaching reductions reached 200 kg C yr^{-1} . On the other hand, groundwater irrigation led to an increase
 326 in surface runoff, which led to an increase in DOC runoff. The most affected areas are characterized by
 327 well-developed agriculture.

328 Figures 6c and 6d show the spatial distribution of the effects of groundwater regulation on river
 329 discharge and DOC export from 1981 to 2013. It can be seen that river discharge significantly decreased
 330 in areas with high groundwater extraction rates, such as the central United States, Pakistan, Afghanistan,
 331 and northern China, resulting in a decrease in riverine DOC export. The largest decrease occurred in the

332 Yangtze River Basin in China, reaching 50 Gg C yr⁻¹; most other rivers were around 10 Gg C yr⁻¹. In
333 addition, although river discharge was reduced in some river sections, soil DOC loss was higher, and
334 DOC export fluxes were still increasing, especially in the lower Yellow River, Mississippi River, and
335 Ganges River basins. This was due to the predominance of agricultural irrigation water in these regions.

336 The amount of carbon flux variation influenced by groundwater regulation was relatively small
337 compared to that influenced by surface water regulation, but there was some interannual fluctuation, with
338 the greatest impact during 2009–2012 (Fig. 7). The intermittent increase and decrease of the variation
339 indicate that river carbon transport fluxes did not decrease directly with increases of groundwater
340 pumping rate, but were also related to the complex carbon and nitrogen cycling processes in terrestrial
341 ecosystems. In addition, irrigation after groundwater extraction from an underground aquifer did not
342 consider directly sending DOC back to the soil carbon pool, and therefore the carbon flux changes were
343 smaller. Because groundwater regulation activities are mostly concentrated in the northern temperate
344 zone, the Pacific and Atlantic regions were the most obviously affected, whereas the remaining regions
345 did not change much.

346 **4.4. Effects of anthropogenic water regulation on riverine DOC transport**

347 This section discusses the combined effects of anthropogenic water regulation on soil and riverine carbon
348 transport using the EXPB minus CTL results. The effects of anthropogenic water regulation on total
349 runoff both increased and decreased globally (Fig. 9f). The western United States, Venezuela, and
350 northern China showed an increase in runoff due to the high intensity of irrigation water use in agriculture.
351 In contrast, regions such as northern India and the central United States showed a decrease in runoff due
352 to frequent groundwater extraction. Overall, human water regulation activities led to an increase in latent
353 heat fluxes and soil moisture and a decrease in sensible heat fluxes and in soil and ground temperatures.

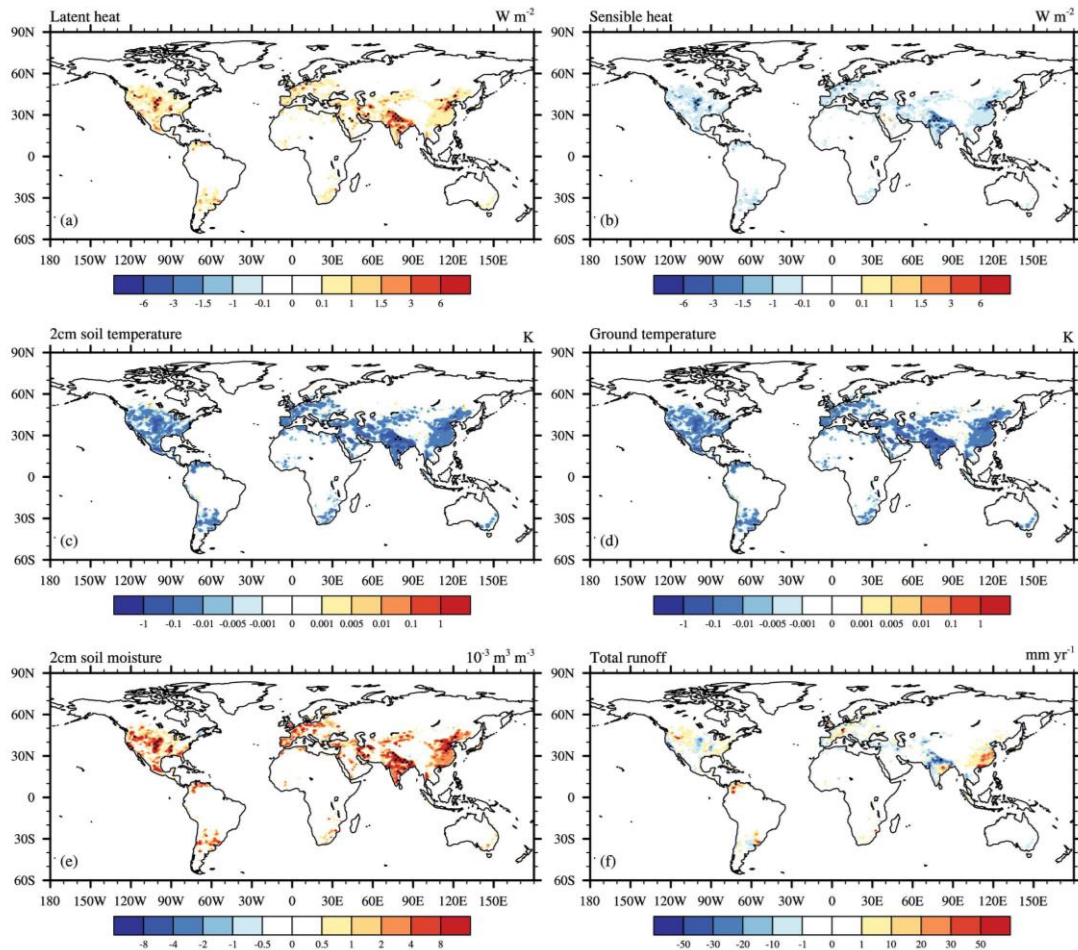


Figure 9. Spatial distribution of multi-year average differences in land surface hydrological variables between EXPB and CTL from 1981 to 2013: (a) latent heat flux, (b) sensible heat flux, (c) 2 cm soil temperature, (d) surface temperature, (e) 2 cm soil moisture, (f) total runoff. This figure demonstrates the effects of anthropogenic water regulation on land surface hydrological variables. The black dots are the regions that pass the significance *t*-test at the 95 % confidence level.

354 Figure 5e shows that soil DOC runoff increased, especially in northern China and the midwestern
 355 United States. DOC leaching decreased in some river sections (Fig. 5f), but not significantly. Although
 356 soil DOC runoff showed an overall increase, DOC export fluxes decreased in most rivers globally due to
 357 water regulation (Fig. 6f). On the one hand, human water use activities led to a decrease in river discharge
 358 (Fig. 6e), and on the other hand, reservoirs have intercepted part of riverine DOC, which led to an increase
 359 in microbial activity, resulting in a decrease in river carbon flux. In contrast, in the Mississippi and
 360 Ganges River basins, although groundwater regulation increased their DOC export fluxes (Fig. 6d), they
 361 still showed a decrease under the negative feedback effect of surface water regulation, indicating that
 362 most rivers globally are mainly influenced by reservoir interception and surface water withdrawal.

363 Five typical rivers were selected to exhibit how anthropogenic water regulation affects monthly and
364 annual average DOC flows in rivers. The selected rivers were the Mississippi River in the United States,
365 the Danube River in Europe, the Ob River in Russia, the Yangtze River in China, and the Ganges River
366 in India. Figure 10 displays the seasonal and interannual variation of DOC flow rates in the five rivers as
367 calculated by the three sets of simulations respectively. Anthropogenic water regulation had a significant
368 impact on the Mississippi, Danube, Yangtze, and Ganges Rivers, which decreased significantly in winter
369 and early spring, whereas the Ob River was almost unaffected. This was the case because of weak water
370 management activities in the Ob River, whereas the other subtropical and temperate rivers had intense
371 water management activities and significant seasonal variation in runoff. In addition, only the Mississippi,
372 Yangtze, and Ganges rivers were affected by minor groundwater regulation, usually occurring during dry
373 periods, whereas in most seasons, the rivers were affected only by surface water regulation (including
374 reservoir interception). The annual results showed a significantly strengthening trend of riverine DOC
375 reduction due to the influence of anthropogenic water regulation, especially in the Danube and Yangtze
376 Rivers, where the retention percentage in 2013 was four to five times higher than in 1981, up to more
377 than 50 %, indicating a clear intensification of human water management activities. The influence on the
378 Mississippi and Ganges Rivers increased slightly and stabilized at about 30–40 %, whereas the influence
379 on the Ob River was almost 0.

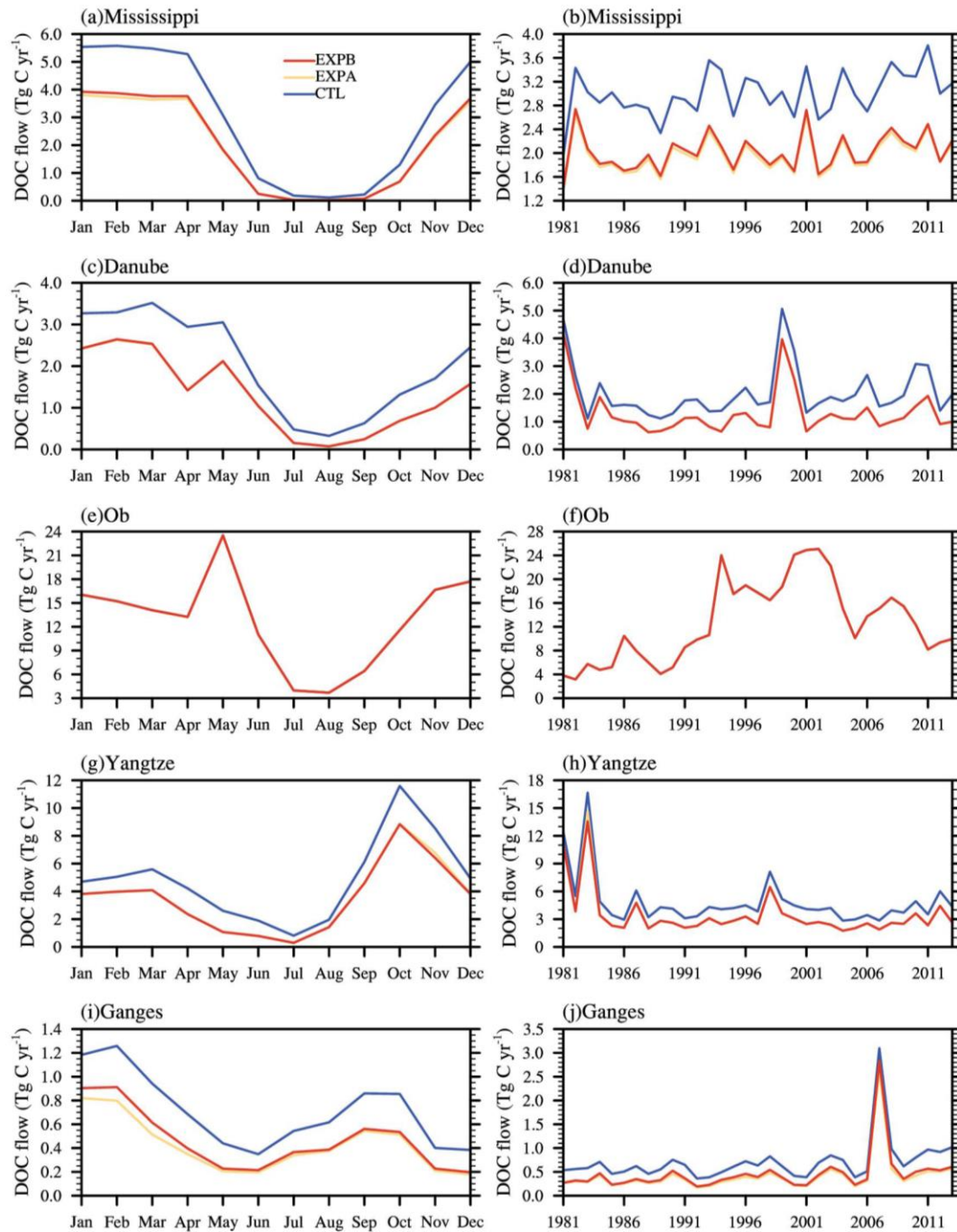


Figure 10. Time series of (a, c, e, g, i) monthly and (b, d, f, h, j) annual average riverine DOC flow rates for the five typical rivers simulated by CTL (blue line), EXPA (yellow line), and EXPB (red line): (a, b) Mississippi River (32.25° N, 91.25° W), (c, d) Danube River (45.25° N, 28.75° E), (e, f) Ob River (66.25° N, 66.75° E), (g, h) Yangtze River (30.75° N, 117.75° E), (i, j) Ganges River (24.25° N, 88.25° E).

380 Riverine DOC export fluxes have obvious spatial heterogeneity. Six zones were defined according to
 381 the latitudes where the river mouths are located, and the effects of the presence or absence of
 382 anthropogenic water regulation on DOC export fluxes are shown in Fig. 11. The hotspot regions of

383 riverine DOC export are concentrated in the tropics (23.5° S–23.5° N) and the mid and high latitudes of
 384 the Northern Hemisphere (40–90° N). The DOC export fluxes of rivers between 40° N and 66° N
 385 accounted for 35.32 % of total global export flux. Due to anthropogenic water regulation, the global DOC
 386 export flux was reduced by 13.36 ± 2.45 Tg C yr⁻¹ compared to the case with no human regulation, with
 387 the greatest impact concentrated in the subtropical and temperate regions of the Northern Hemisphere
 388 (23.5–66° N) because this is the region with the highest intensity of human water use activity.

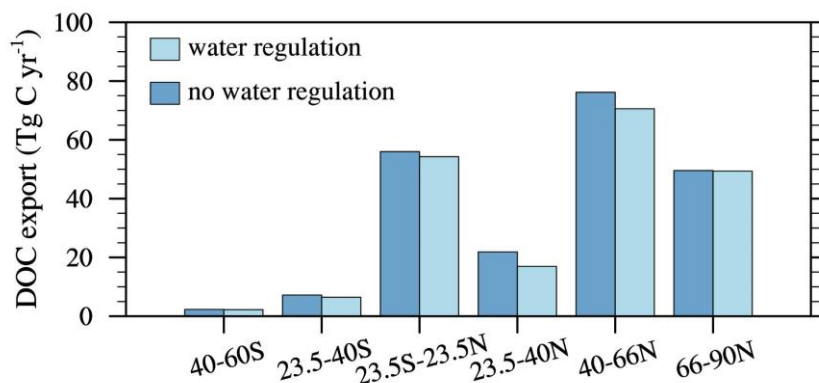


Figure 11. Bar chart of latitudinal band distribution of multi-year average DOC export fluxes from 1981 to 2013. Dark blue indicates no water regulation, and light blue indicates anthropogenic water regulation.

389 Overall, anthropogenic water regulation reduced global riverine carbon fluxes, and the reduction in
 390 DOC fluxes also intensified over time, from -9.13 Tg C yr⁻¹ to -16.45 Tg C yr⁻¹ (Fig. 12), and the
 391 reduction percentage also increased from 4.83 % to 6.20 %. Rivers in the Pacific and Atlantic regions
 392 were more affected by water regulation, and the interannual changes were more consistent with the global
 393 picture. The flux of rivers into the Indian Ocean, which was reduced by water regulation, was about 1.27
 394 ± 0.23 Tg C yr⁻¹, which was small compared to the global flux, and the flux into the Arctic Ocean was
 395 almost negligible due to the scarcity of human activities.

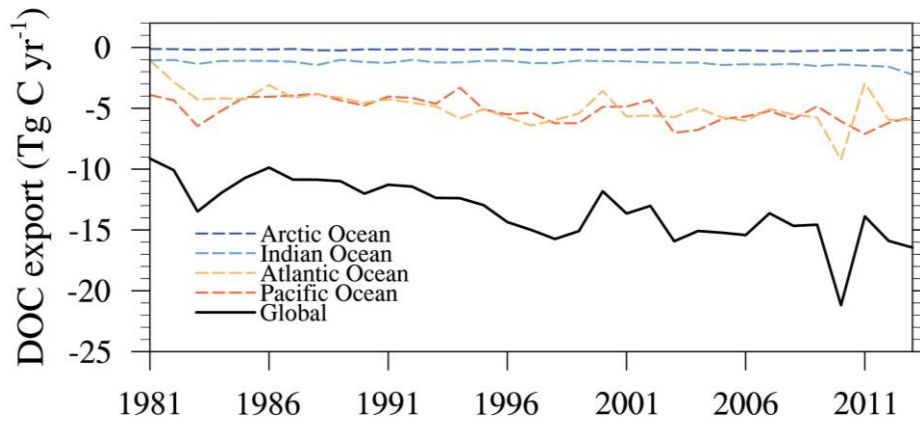


Figure 12. Interannual variability in the impact of anthropogenic water regulation on riverine DOC delivery from rivers to the ocean.

396 **5. Conclusions**

397 This study has developed schemes that consider soil and riverine DOC dynamics and anthropogenic
 398 water regulation activities and has incorporated them into the land surface model CLM5.0. The simulated
 399 river discharges and riverine DOC export fluxes were in good agreement with observations obtained for
 400 106 major world rivers. Surface water and groundwater use datasets were used as inputs to the model,
 401 and three sets of numerical simulations were conducted from 1981 to 2013 on a global scale to investigate
 402 the effects of anthropogenic water regulation on riverine DOC transport.

403 The main conclusions of this study are as follows. First, anthropogenic water regulation activities
 404 increased soil losses in most arid and semi-arid regions of the world, although groundwater extraction
 405 reduced subsurface runoff and decreased DOC leaching; however, this decrease was less than the increase
 406 in DOC runoff due to irrigation. Second, the DOC export fluxes of the Yangtze, Yellow, Mississippi, and
 407 Ganges River basins were significantly reduced by reservoir regulation and surface water withdrawal.
 408 However, DOC export fluxes in these areas showed an increase under groundwater regulation, but the
 409 increase was small, indicating that DOC transport in most rivers globally is mainly influenced by
 410 reservoir interception and surface water regulation. Third, further analysis showed that subtropical and
 411 temperate rivers with intensive water management regimes were more affected and that DOC flows
 412 decreased substantially in winter and early spring. The retention percentage has been increasing year by
 413 year, up to over 50 %, indicating a clear intensification of human water management activities, especially
 414 along the Danube and Yangtze Rivers. In addition, the greatest impact of anthropogenic water regulation

415 activities was concentrated in the region from 23.5°N to 66°N because this zone contains the highest
416 intensity of human water use activities. Fourth, global riverine DOC flux transport to the ocean decreased
417 by an average of 13.36 ± 2.45 Tg C yr⁻¹ per year due to anthropogenic water regulation activities, and
418 the decrease in DOC flux became more pronounced with time, from -9.13 Tg C yr⁻¹ (4.83 %) in 1981 to
419 -16.45 Tg C yr⁻¹ (6.20 %) in 2013, especially in the Pacific and Atlantic Ocean regions. Meanwhile, the
420 Arctic Ocean region was almost unaffected due to low anthropogenic disturbance. In general, this study
421 has developed an effective scheme to simulate DOC export from terrestrial to aquatic systems, which is
422 important for improving carbon budget estimation and integrated ecosystem management.

423 However, there are still some limitations and uncertainties in the developed model that need to be
424 addressed in the future. In this study, we evaluated global riverine DOC transport using observations
425 from a limited number of river sites in literature records, which may have induced a bias. Besides, the
426 simplification of the carbon dynamics of soils and rivers, the uniform parameters, and input data sets also
427 produce some uncertainties. To advance the current model, more observed data sets and more complex
428 schemes of carbon dynamics are needed. In addition, other human activities, such as fertilization,
429 wastewater discharge, and land use change, have a significant impact on riverine carbon transport
430 (Regnier et al., 2013), and should be considered in our future work.

431
432 **Code and Data Availability.** The observed river discharge and riverine DOC exports data can be available
433 through Dai et al. (2012). The source code of CLM 5.0 is available online
434 (<https://www.cesm.ucar.edu/models/clm>). The FORTRAN code of developed model in this study is
435 available upon request. Please contact Zhenghui Xie at zxie@lasg.iap.ac.cn. The drawing language is the
436 NCL language.

437
438 **Author contributions.** The scientific framing of this paper was developed by YY, ZX, BJ. The model
439 was initiated by YY and YW. The literature review was performed by HY, YT and SC. Analyses and
440 scientific post-processing were performed by LW and RL. All authors discussed the results and
441 contributed to the writing of the paper.

442
443 **Competing interests.** The contact author has declared that neither they nor their co-authors have any
444 competing interests.

445 ***Acknowledgments.*** This work was jointly supported by the National Key Research and Development
446 Program of China (grant number: 2022YFC3201903), the National Natural Science Foundation of China
447 (grant number: 41830967), the Youth Innovation Promotion Association CAS (2021073), the National
448 Key Scientific and Technological Infrastructure project “Earth System Science Numerical Simulator
449 Facility” (EarthLab), and the National Natural Science Foundation of China (grant number: 42175163).
450 We would like to thank the editor and the three anonymous reviewers for their constructive and thoughtful
451 comments.

452 **References**

- 453 Aitkenhead, J. A. and McDowell, W. H.: Soil C:N ratio as a predictor of annual riverine DOC flux at
454 local and global scales, *Global Biogeochem. Cycles*, 14, 127–138,
455 <https://doi.org/10.1029/1999GB900083>, 2000.
- 456 Cai, W.: Estuarine and Coastal Ocean Carbon Paradox: CO₂ Sinks or Sites of Terrestrial Carbon
457 Incineration?, *Annu. Rev. Mar. Sci.*, 3, 123–145, <https://doi.org/10.1146/annurev-marine-120709-142723>, 2011.
- 459 Camino-Serrano, M., Guenet, B., Luysaert, S., Ciais, P., Bastrikov, V., De Vos, B., Gielen, B., Gleixner,
460 G., Jornet-Puig, A., Kaiser, K., Kothawala, D., Lauerwald, R., Peñuelas, J., Schrumppf, M., Vicca, S.,
461 Vuichard, N., Walmsley, D., and Janssens, I. A.: ORCHIDEE-SOM: modeling soil organic carbon (SOC)
462 and dissolved organic carbon (DOC) dynamics along vertical soil profiles in Europe, *Geosci. Model Dev.*,
463 11, 937–957, <https://doi.org/10.5194/gmd-11-937-2018>, 2018.
- 464 Cole, J. J., Prairie, Y. T., Caraco, N. F., McDowell, W. H., Tranvik, L. J., Striegl, R. G., Duarte, C. M.,
465 Kortelainen, P., Downing, J. A., Middelburg, J. J., and Melack, J.: Plumbing the Global Carbon Cycle:
466 Integrating Inland Waters into the Terrestrial Carbon Budget, *Ecosystems*, 10, 172–185,
467 <https://doi.org/10.1007/s10021-006-9013-8>, 2007.
- 468 Dai, M., Yin, Z., Meng, F., Liu, Q., and Cai, W.-J.: Spatial distribution of riverine DOC inputs to the
469 ocean: an updated global synthesis, *Current Opinion in Environmental Sustainability*, 4, 170–178,
470 <https://doi.org/10.1016/j.cosust.2012.03.003>, 2012.
- 471 Drake, T. W., Raymond, P. A., and Spencer, R. G. M.: Terrestrial carbon inputs to inland waters: A current
472 synthesis of estimates and uncertainty, *Limnol Oceanogr Lett*, 3, 132–142,
473 <https://doi.org/10.1002/lol2.10055>, 2018.
- 474 Fabre, C., Sauvage, S., Probst, J.-L., and Sánchez-Pérez, J. M.: Global-scale daily riverine DOC fluxes
475 from lands to the oceans with a generic model, *Global and Planetary Change*, 194, 103294,
476 <https://doi.org/10.1016/j.gloplacha.2020.103294>, 2020.
- 477 Futter, M. N., Butterfield, D., Cosby, B. J., Dillon, P. J., Wade, A. J., and Whitehead, P. G.: Modeling the
478 mechanisms that control in-stream dissolved organic carbon dynamics in upland and forested catchments:
479 MODELING SURFACE WATER DOC, *Water Resour. Res.*, 43,
480 <https://doi.org/10.1029/2006WR004960>, 2007.
- 481 Gerber, S., Hedin, L. O., Oppenheimer, M., Pacala, S. W., and Shevliakova, E.: Nitrogen cycling and
482 feedbacks in a global dynamic land model, *Global Biogeochem. Cycles*, 24,
483 <https://doi.org/10.1029/2008GB003336>, 2010.
- 484 Gommet, C., Lauerwald, R., Ciais, P., Guenet, B., Zhang, H., and Regnier, P.: Spatiotemporal patterns
485 and drivers of terrestrial dissolved organic carbon (DOC) leaching into the European river network, *Earth
486 Syst. Dynam.*, 13, 393–418, <https://doi.org/10.5194/esd-13-393-2022>, 2022.
- 487 Hanasaki, N., Kanae, S., and Oki, T.: A reservoir operation scheme for global river routing models,

488 Journal of Hydrology, 327, 22–41, <https://doi.org/10.1016/j.jhydrol.2005.11.011>, 2006.

489 Harrison, J. A., Caraco, N., and Seitzinger, S. P.: Global patterns and sources of dissolved organic matter
490 export to the coastal zone: Results from a spatially explicit, global model: GLOBAL DISSOLVED
491 ORGANIC MATTER EXPORT, *Global Biogeochem. Cycles*, 19, n/a-n/a,
492 <https://doi.org/10.1029/2005GB002480>, 2005.

493 van Hoek, W. J., Wang, J., Vilmin, L., Beusen, A. H. W., Mogollón, J. M., Müller, G., Pika, P. A., Liu,
494 X., Langeveld, J. J., Bouwman, A. F., and Middelburg, J. J.: Exploring Spatially Explicit Changes in
495 Carbon Budgets of Global River Basins during the 20th Century, *Environ. Sci. Technol.*, 55, 16757–
496 16769, <https://doi.org/10.1021/acs.est.1c04605>, 2021.

497 Janssens, I. A. and Pilegaard, K.: Large seasonal changes in Q_{10} of soil respiration in a beech forest:
498 SHORT-TERM Q_{10} OF SOIL RESPIRATION, *Global Change Biology*, 9, 911–918,
499 <https://doi.org/10.1046/j.1365-2486.2003.00636.x>, 2003.

500 Lawrence, D., Fisher, R., and Koven, C.: Technical Description of version 5.0 of the Community Land
501 Model (CLM), NCAR, NCAR, Boulder, US, 2018.

502 Lehner, B., Liermann, C. R., Revenga, C., Vörösmarty, C., Fekete, B., Crouzet, P., Döll, P., Endejan, M.,
503 Frenken, K., Magome, J., Nilsson, C., Robertson, J. C., Rödel, R., Sindorf, N., and Wisser, D.: High-
504 resolution mapping of the world's reservoirs and dams for sustainable river-flow management, *Frontiers
505 in Ecology and the Environment*, 9, 494–502, <https://doi.org/10.1890/100125>, 2011.

506 Li, H., Wigmosta, M. S., Wu, H., Huang, M., Ke, Y., Coleman, A. M., and Leung, L. R.: A Physically
507 Based Runoff Routing Model for Land Surface and Earth System Models, *Journal of Hydrometeorology*,
508 14, 808–828, <https://doi.org/10.1175/JHM-D-12-015.1>, 2013.

509 Li, M., Peng, C., Zhou, X., Yang, Y., Guo, Y., Shi, G., and Zhu, Q.: Modeling Global Riverine DOC Flux
510 Dynamics From 1951 to 2015, *J. Adv. Model. Earth Syst.*, 11, 514–530,
511 <https://doi.org/10.1029/2018MS001363>, 2019.

512 Liao, C., Zhuang, Q., Leung, L. R., and Guo, L.: Quantifying Dissolved Organic Carbon Dynamics Using
513 a Three-Dimensional Terrestrial Ecosystem Model at High Spatial-Temporal Resolutions, *J. Adv. Model.
514 Earth Syst.*, 11, 4489–4512, <https://doi.org/10.1029/2019MS001792>, 2019.

515 Liu, S., Xie, Z., Zeng, Y., Liu, B., Li, R., Wang, Y., Wang, L., Qin, P., Jia, B., and Xie, J.: Effects of
516 anthropogenic nitrogen discharge on dissolved inorganic nitrogen transport in global rivers, *Glob Change
517 Biol*, 25, 1493–1513, <https://doi.org/10.1111/gcb.14570>, 2019.

518 Liu, S., Xie, Z., Liu, B., Wang, Y., Gao, J., Zeng, Y., Xie, J., Xie, Z., Jia, B., Qin, P., Li, R., Wang, L., and
519 Chen, S.: Global river water warming due to climate change and anthropogenic heat emission, *Global
520 and Planetary Change*, 193, 103289, <https://doi.org/10.1016/j.gloplacha.2020.103289>, 2020.

521 Liu, S., Maavara, T., Brinkerhoff, C. B., and Raymond, P. A.: Global Controls on DOC Reaction Versus
522 Export in Watersheds: A Damköhler Number Analysis, *Global Biogeochemical Cycles*, 36,
523 <https://doi.org/10.1029/2021GB007278>, 2022.

- 524 Ludwig, W., Probst, J.-L., and Kempe, S.: Predicting the oceanic input of organic carbon by continental
525 erosion, *Global Biogeochem. Cycles*, 10, 23–41, <https://doi.org/10.1029/95GB02925>, 1996.
- 526 Maavara, T., Lauerwald, R., Regnier, P., and Van Cappellen, P.: Global perturbation of organic carbon
527 cycling by river damming, *Nat Commun*, 8, 15347, <https://doi.org/10.1038/ncomms15347>, 2017.
- 528 Meybeck, M.: Carbon, nitrogen, and phosphorus transport by world rivers, *American Journal of Science*,
529 282, 401–450, <https://doi.org/10.2475/ajs.282.4.401>, 1982.
- 530 Meybeck, M. and Ragu, A.: GEMS-GLORI world river discharge database,
531 <https://doi.org/10.1594/PANGAEA.804574>, 2012.
- 532 Neff, J. C. and Asner, G. P.: Dissolved Organic Carbon in Terrestrial Ecosystems: Synthesis and a Model,
533 *Ecosystems*, 4, 29–48, <https://doi.org/10.1007/s100210000058>, 2001.
- 534 Oleson, K. W., Lawrence, D. M., and Bonan, G. B.: Technical Description of version 4.5 of the
535 Community Land Model (CLM), NCAR, NCAR, Boulder, US, 2013.
- 536 Parton, W. J., Stewart, J. W. B., and Cole, C. V.: Dynamics of C, N, P and S in Grassland Soils: A Model,
537 *Biogeochemistry*, 5, 109–131, <https://doi.org/10.1007/BF02180320>, 1988.
- 538 Regnier, P., Friedlingstein, P., Ciais, P., Mackenzie, F. T., Gruber, N., Janssens, I. A., Laruelle, G. G.,
539 Lauerwald, R., Luysaert, S., Andersson, A. J., Arndt, S., Arnosti, C., Borges, A. V., Dale, A. W., Gallego-
540 Sala, A., Godd eris, Y., Goossens, N., Hartmann, J., Heinze, C., Ilyina, T., Joos, F., LaRowe, D. E., Leifeld,
541 J., Meysman, F. J. R., Munhoven, G., Raymond, P. A., Spahni, R., Suntharalingam, P., and Thullner, M.:
542 Anthropogenic perturbation of the carbon fluxes from land to ocean, *Nature Geosci*, 6, 597–607,
543 <https://doi.org/10.1038/ngeo1830>, 2013.
- 544 Ren, W., Tian, H., Cai, W.-J., Lohrenz, S. E., Hopkinson, C. S., Huang, W.-J., Yang, J., Tao, B., Pan, S.,
545 and He, R.: Century-long increasing trend and variability of dissolved organic carbon export from the
546 Mississippi River basin driven by natural and anthropogenic forcing: Export of DOC from the
547 Mississippi River, *Global Biogeochem. Cycles*, 30, 1288–1299, <https://doi.org/10.1002/2016GB005395>,
548 2016.
- 549 Seitzinger, S. P., Harrison, J. A., Dumont, E., Beusen, A. H. W., and Bouwman, A. F.: Sources and
550 delivery of carbon, nitrogen, and phosphorus to the coastal zone: An overview of Global Nutrient Export
551 from Watersheds (NEWS) models and their application., *Global Biogeochem. Cycles*, 19,
552 <https://doi.org/10.1029/2005GB002606>, 2005.
- 553 Siebert, S., Henrich, V., Frenken, K., and Burke, J.: Update of the digital global map of irrigation areas
554 to version 5., <https://doi.org/10.13140/2.1.2660.6728>, 2013.
- 555 Smith, S. V. and Hollibaugh, J. T.: Coastal metabolism and the oceanic organic carbon balance, *Rev.*
556 *Geophys.*, 31, 75–89, <https://doi.org/10.1029/92RG02584>, 1993.
- 557 Tian, H., Yang, Q., Najjar, R. G., Ren, W., Friedrichs, M. A. M., Hopkinson, C. S., and Pan, S.:
558 Anthropogenic and climatic influences on carbon fluxes from eastern North America to the Atlantic

559 Ocean: A process-based modeling study, *J. Geophys. Res. Biogeosci.*, 120, 757–772,
560 <https://doi.org/10.1002/2014JG002760>, 2015.

561 Tranvik, L. J. and Jansson, M.: Terrestrial export of organic carbon, *Nature*, 415, 861–862,
562 <https://doi.org/10.1038/415861b>, 2002.

563 Viovy, N.: CRUNCEP Version 7 - Atmospheric Forcing Data for the Community Land Model,
564 <https://doi.org/10.5065/PZ8F-F017>, 2018.

565 van Vliet, M. T. H., Yearsley, J. R., Franssen, W. H. P., Ludwig, F., Haddeland, I., Lettenmaier, D. P., and
566 Kabat, P.: Coupled daily streamflow and water temperature modelling in large river basins, *Hydrology
567 and Earth System Sciences*, 16, 4303–4321, <https://doi.org/10.5194/hess-16-4303-2012>, 2012.

568 Wang, Y., Xie, Z., Liu, S., Wang, L., Li, R., Chen, S., Jia, B., Qin, P., and Xie, J.: Effects of Anthropogenic
569 Disturbances and Climate Change on Riverine Dissolved Inorganic Nitrogen Transport, *Journal of
570 Advances in Modeling Earth Systems*, 12, e2020MS002234, <https://doi.org/10.1029/2020MS002234>,
571 2020.

572 Wu, H., Peng, C., Moore, T. R., Hua, D., Li, C., Zhu, Q., Peichl, M., Arain, M. A., and Guo, Z.: Modeling
573 dissolved organic carbon in temperate forest soils: TRIPLEX-DOC model development and validation,
574 *Geosci. Model Dev.*, 7, 867–881, <https://doi.org/10.5194/gmd-7-867-2014>, 2014.

575 Xie, Z., Wang, L., Wang, Y., Liu, B., Li, R., Xie, J., Zeng, Y., Liu, S., Gao, J., Chen, S., Jia, B., and Qin,
576 P.: Land Surface Model CAS-LSM: Model Description and Evaluation, *Journal of Advances in Modeling
577 Earth Systems*, 12, e2020MS002339, <https://doi.org/10.1029/2020MS002339>, 2020.

578 Yao, Y., Tian, H., Pan, S., Najjar, R. G., Friedrichs, M. A. M., Bian, Z., Li, H., and Hofmann, E. E.:
579 Riverine Carbon Cycling Over the Past Century in the Mid-Atlantic Region of the United States, *J
580 Geophys Res Biogeosci.*, 126, <https://doi.org/10.1029/2020JG005968>, 2021.

581 Yearsley, J.: A semi-Lagrangian water temperature model for advection-dominated river systems, *Water
582 Resources Research - WATER RESOUR RES.*, 45, <https://doi.org/10.1029/2008WR007629>, 2009.

583 Zeng, Y., Xie, Z., Yu, Y., Liu, S., Wang, L., Zou, J., Qin, P., and Jia, B.: Effects of anthropogenic water
584 regulation and groundwater lateral flow on land processes, *Journal of Advances in Modeling Earth
585 Systems*, 8, 1106–1131, <https://doi.org/10.1002/2016MS000646>, 2016.

586 Zeng, Y., Xie, Z., and Zou, J.: Hydrologic and Climatic Responses to Global Anthropogenic Groundwater
587 Extraction, *Journal of Climate*, 30, 71–90, <https://doi.org/10.1175/JCLI-D-16-0209.1>, 2017.

588 Zhang, Y.: The review of the research of the riverine organic carbon cycle, *Journal of Henan Polytechnic
589 University(Natural Science)*, 31, 344–351, <https://doi.org/10.16186/j.cnki.1673-9787.2012.03.006>,
590 2012.

591 Zou, J., Xie, Z., Yu, Y., Zhan, C., and Sun, Q.: Climatic responses to anthropogenic groundwater
592 exploitation: a case study of the Haihe River Basin, Northern China, *Clim Dyn.*, 42, 2125–2145,
593 <https://doi.org/10.1007/s00382-013-1995-2>, 2014.

594 Zou, J., Xie, Z., Zhan, C., Qin, P., Sun, Q., Jia, B., and Xia, J.: Effects of anthropogenic groundwater
595 exploitation on land surface processes: A case study of the Haihe River Basin, northern China, *Journal*
596 *of Hydrology*, 524, 625–641, <https://doi.org/10.1016/j.jhydrol.2015.03.026>, 2015.

597